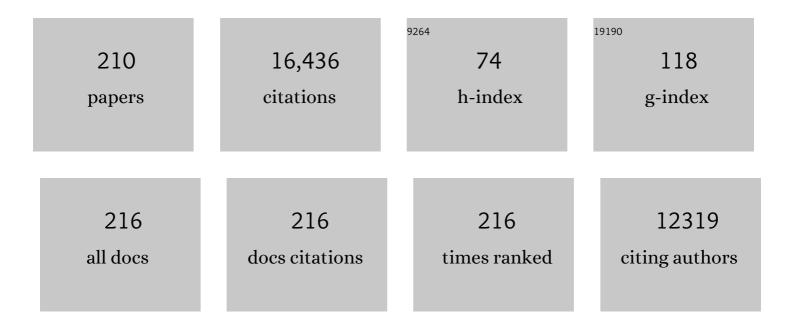
Ruben Kretzschmar

List of Publications by Year in descending order

Source: https://exaly.com/author-pdf/8419900/publications.pdf Version: 2024-02-01



#	Article	IF	CITATIONS
1	Biogeochemical Redox Processes and their Impact on Contaminant Dynamics. Environmental Science & Technology, 2010, 44, 15-23.	10.0	1,037
2	Mobile Subsurface Colloids and Their Role in Contaminant Transport. Advances in Agronomy, 1999, 66, 121-193.	5.2	531
3	Quantitative antimony speciation in shooting-range soils by EXAFS spectroscopy. Geochimica Et Cosmochimica Acta, 2006, 70, 3299-3312.	3.9	282
4	Experimental determination of colloid deposition rates and collision efficiencies in natural porous media. Water Resources Research, 1997, 33, 1129-1137.	4.2	257
5	Mercury Deposition and Re-emission Pathways in Boreal Forest Soils Investigated with Hg Isotope Signatures. Environmental Science & Technology, 2015, 49, 7188-7196.	10.0	242
6	Changes in Zinc Speciation in Field Soil after Contamination with Zinc Oxide. Environmental Science & amp; Technology, 2005, 39, 6616-6623.	10.0	235
7	Iron Isotope Fractionation during Proton-Promoted, Ligand-Controlled, and Reductive Dissolution of Goethite. Environmental Science & Technology, 2006, 40, 3787-3793.	10.0	235
8	Spectroscopic Evidence for Ternary Complex Formation between Arsenate and Ferric Iron Complexes of Humic Substances. Environmental Science & amp; Technology, 2011, 45, 9550-9557.	10.0	234
9	Transport of Humic-Coated Iron Oxide Colloids in a Sandy Soil:Â Influence of Ca2+and Trace Metals. Environmental Science & Technology, 1997, 31, 3497-3504.	10.0	233
10	Equilibrium Mercury Isotope Fractionation between Dissolved Hg(II) Species and Thiol-Bound Hg. Environmental Science & Technology, 2010, 44, 4191-4197.	10.0	230
11	Soil Biogeochemical Processes within the Critical Zone. Elements, 2007, 3, 321-326.	0.5	224
12	Redox-Controlled Changes in Cadmium Solubility and Solid-Phase Speciation in a Paddy Soil As Affected by Reducible Sulfate and Copper. Environmental Science & Technology, 2013, 47, 12775-12783.	10.0	222
13	Transport of in Situ Mobilized Colloidal Particles in Packed Soil Columns. Environmental Science & Technology, 1998, 32, 3562-3569.	10.0	219
14	Combining Selective Sequential Extractions, X-ray Absorption Spectroscopy, and Principal Component Analysis for Quantitative Zinc Speciation in Soil. Environmental Science & Technology, 2002, 36, 5021-5028.	10.0	215
15	Absolute Aggregation Rate Constants of Hematite Particles in Aqueous Suspensions: A Comparison of Two Different Surface Morphologies. Journal of Colloid and Interface Science, 1997, 196, 241-253.	9.4	201
16	Arsenic sequestration by organic sulphur in peat. Nature Geoscience, 2012, 5, 66-73.	12.9	201
17	Dissolution mechanisms of goethite in the presence of siderophores and organic acids. Geochimica Et Cosmochimica Acta, 2007, 71, 5635-5650.	3.9	184
18	Influence of pH and Humic Acid on Coagulation Kinetics of Kaolinite: A Dynamic Light Scattering Study, Journal of Colloid and Interface Science, 1998, 202, 95-103	9.4	183

#	Article	IF	CITATIONS
19	Temperature Dependence and Coupling of Iron and Arsenic Reduction and Release during Flooding of a Contaminated Soil. Environmental Science & Technology, 2010, 44, 116-122.	10.0	182
20	Metal Retention and Transport on Colloidal Particles in the Environment. Elements, 2005, 1, 205-210.	0.5	180
21	Spatial Distribution and Temporal Variability of Arsenic in Irrigated Rice Fields in Bangladesh. 2. Paddy Soil. Environmental Science & Technology, 2007, 41, 5967-5972.	10.0	173
22	Contaminant mobilization by metallic copper and metal sulphide colloids in flooded soil. Nature Geoscience, 2009, 2, 267-271.	12.9	167
23	Synthetic coprecipitates of exopolysaccharides and ferrihydrite. Part I: Characterization. Geochimica Et Cosmochimica Acta, 2008, 72, 1111-1127.	3.9	165
24	Effects of Adsorbed Humic Acid on Surface Charge and Flocculation of Kaolinite. Soil Science Society of America Journal, 1997, 61, 101-108.	2.2	163
25	Relating Ion Binding by Fulvic and Humic Acids to Chemical Composition and Molecular Size. 2. Metal Binding. Environmental Science & Technology, 2001, 35, 2512-2517.	10.0	158
26	Chemical and Biological Gradients along the Damma Glacier Soil Chronosequence, Switzerland. Vadose Zone Journal, 2011, 10, 867-883.	2.2	158
27	Multi-metal contaminant dynamics in temporarily flooded soil under sulfate limitation. Geochimica Et Cosmochimica Acta, 2009, 73, 5513-5527.	3.9	149
28	Chemical Heterogeneity of Organic Soil Colloids Investigated by Scanning Transmission X-ray Microscopy and C-1s NEXAFS Microspectroscopy. Environmental Science & Technology, 2005, 39, 9094-9100.	10.0	147
29	Distribution and speciation of arsenic around roots in a contaminated riparian floodplain soil: Micro-XRF element mapping and EXAFS spectroscopy. Geochimica Et Cosmochimica Acta, 2007, 71, 5804-5820.	3.9	145
30	Control of arsenic mobilization in paddy soils by manganese and iron oxides. Environmental Pollution, 2017, 231, 37-47.	7.5	145
31	Solution Speciation Controls Mercury Isotope Fractionation of Hg(II) Sorption to Goethite. Environmental Science & Technology, 2012, 46, 6654-6662.	10.0	143
32	Combining spectroscopic and isotopic techniques gives a dynamic view of phosphorus cycling in soil. Nature Communications, 2018, 9, 3226.	12.8	141
33	Impact of Organic Matter on Iron(II)-Catalyzed Mineral Transformations in Ferrihydrite–Organic Matter Coprecipitates. Environmental Science & Technology, 2018, 52, 12316-12326.	10.0	139
34	Relating Ion Binding by Fulvic and Humic Acids to Chemical Composition and Molecular Size. 1. Proton Binding. Environmental Science & Technology, 2001, 35, 2505-2511.	10.0	135
35	Spatial Distribution and Temporal Variability of Arsenic in Irrigated Rice Fields in Bangladesh. 1. Irrigation Water. Environmental Science & Technology, 2007, 41, 5960-5966.	10.0	132
36	Arsenic release from paddy soils during monsoonÂflooding. Nature Geoscience, 2010, 3, 53-59.	12.9	123

3

#	Article	IF	CITATIONS
37	Interaction of copper and fulvic acid at the hematite-water interface. Geochimica Et Cosmochimica Acta, 2001, 65, 3435-3442.	3.9	120
38	Iron isotope fractionation in oxic soils by mineral weathering and podzolization. Geochimica Et Cosmochimica Acta, 2007, 71, 5821-5833.	3.9	118
39	Influence of Natural Organic Matter on Colloid Transport Through Saprolite. Water Resources Research, 1995, 31, 435-445.	4.2	117
40	Competitive sorption of carbonate and arsenic to hematite: Combined ATR-FTIR and batch experiments. Journal of Colloid and Interface Science, 2012, 377, 313-321.	9.4	116
41	Transport of Iron Oxide Colloids in Packed Quartz Sand Media: Monolayer and Multilayer Deposition. Journal of Colloid and Interface Science, 2000, 231, 32-41.	9.4	115
42	Competitive sorption of copper and lead at the oxide-water interface: Implications for surface site density. Geochimica Et Cosmochimica Acta, 1999, 63, 2929-2938.	3.9	108
43	Solid solution between Al-ettringite and Fe-ettringite (Ca6[Al1â~'xFex(OH)6]2(SO4)3·26H2O). Cement and Concrete Research, 2009, 39, 482-489.	11.0	107
44	ATR-FTIR Spectroscopy Study of the Influence of pH and Contact Time on the Adhesion of <i>Shewanella putrefaciens</i> Bacterial Cells to the Surface of Hematite. Environmental Science & Technology, 2012, 46, 12848-12855.	10.0	107
45	Long- and short-term effects of crop residues on aluminum toxicity, phosphorus availability and growth of pearl millet in an acid sandy soil. Plant and Soil, 1991, 136, 215-223.	3.7	104
46	Chemical heterogeneity of humic substances: characterization of size fractions obtained by hollowâ€fibre ultrafiltration. European Journal of Soil Science, 2000, 51, 617-625.	3.9	104
47	Influence of citric acid on the hydration of Portland cement. Cement and Concrete Research, 2009, 39, 275-282.	11.0	104
48	Geochemical Aspects of Phytosiderophoreâ€₽romoted Iron Acquisition by Plants. Advances in Agronomy, 2006, 91, 1-46.	5.2	103
49	Solubility of Fe–ettringite (Ca6[Fe(OH)6]2(SO4)3·26H2O). Geochimica Et Cosmochimica Acta, 2008, 72, 1-18.	3.9	101
50	Title is missing!. Journal of Plant Nutrition and Soil Science, 2003, 166, 84-92.	1.9	99
51	Coethite Dissolution in the Presence of Phytosiderophores: Rates, Mechanisms, and the Synergistic Effect of Oxalate. Plant and Soil, 2005, 276, 115-132.	3.7	97
52	C-1s NEXAFS Spectroscopy Reveals Chemical Fractionation of Humic Acid by Cation-Induced Coagulation. Environmental Science & Technology, 2007, 41, 1915-1920.	10.0	97
53	Reduction and Reoxidation of Humic Acid: Influence on Spectroscopic Properties and Proton Binding. Environmental Science & Technology, 2010, 44, 5787-5792.	10.0	95
54	Formation of Zn-rich phyllosilicate, Zn-layered double hydroxide and hydrozincite in contaminated calcareous soils. Geochimica Et Cosmochimica Acta, 2008, 72, 5037-5054.	3.9	94

#	Article	IF	CITATIONS
55	In situ ATR-FTIR spectroscopic analysis of the co-adsorption of orthophosphate and Cd(II) onto hematite. Geochimica Et Cosmochimica Acta, 2013, 117, 53-64.	3.9	94
56	Hydrological control of stream water chemistry in a glacial catchment (Damma Glacier, Switzerland). Chemical Geology, 2011, 285, 215-230.	3.3	92
57	Impacts of <i>Shewanella putrefaciens</i> Strain CN-32 Cells and Extracellular Polymeric Substances on the Sorption of As(V) and As(III) on Fe(III)-(Hydr)oxides. Environmental Science & Technology, 2011, 45, 2804-2810.	10.0	91
58	Spatial Distribution and Speciation of Lead around Corroding Bullets in a Shooting Range Soil Studied by Micro-X-ray Fluorescence and Absorption Spectroscopy. Environmental Science & Technology, 2005, 39, 4808-4815.	10.0	90
59	Iron isotope fractionation during proton- and ligand-promoted dissolution of primary phyllosilicates. Geochimica Et Cosmochimica Acta, 2010, 74, 3112-3128.	3.9	90
60	Reaction-Based Model Describing Competitive Sorption and Transport of Cd, Zn, and Ni in an Acidic Soil. Environmental Science & amp; Technology, 2001, 35, 1651-1657.	10.0	89
61	Detrital and pedogenic magnetic mineral phases in the loess/palaeosol sequence at Lingtai (Central) Tj ETQq1 1 ().784314 1.9	rgBT /Overlo
62	Soil properties controlling Zn speciation and fractionation in contaminated soils. Geochimica Et Cosmochimica Acta, 2009, 73, 5256-5272.	3.9	88
63	Calcium isotopes in a proglacial weathering environment: Damma glacier, Switzerland. Geochimica Et Cosmochimica Acta, 2011, 75, 106-118.	3.9	88
64	Competitive sorption of protons and metal cations onto kaolinite: experiments and modeling. Journal of Colloid and Interface Science, 2005, 282, 270-282.	9.4	87
65	Assessment of Long-Term Performance and Chromate Reduction Mechanisms in a Field Scale Permeable Reactive Barrier. Environmental Science & amp; Technology, 2009, 43, 6786-6792.	10.0	87
66	Bisulfide Reaction with Natural Organic Matter Enhances Arsenite Sorption: Insights from X-ray Absorption Spectroscopy. Environmental Science & Technology, 2012, 46, 11788-11797.	10.0	87
67	Effect of Humic and Fulvic Acid Concentrations and Ionic Strength on Copper and Lead Binding. Environmental Science & Technology, 2005, 39, 5319-5326.	10.0	86
68	Flocculation of Kaolinitic Soil Clays: Effects of Humic Substances and Iron Oxides. Soil Science Society of America Journal, 1993, 57, 1277-1283.	2.2	83
69	Arsenic in Soil and Irrigation Water Affects Arsenic Uptake by Rice: Complementary Insights from Field and Pot Studies. Environmental Science & Technology, 2010, 44, 8842-8848.	10.0	80
70	Arsenite Binding to Natural Organic Matter: Spectroscopic Evidence for Ligand Exchange and Ternary Complex Formation. Environmental Science & Technology, 2013, 47, 12165-12173.	10.0	80
71	Formation and Dissolution of Single and Mixed Zn and Ni Precipitates in Soil:Â Evidence from Column Experiments and Extended X-ray Absorption Fine Structure Spectroscopy. Environmental Science & Technology, 2005, 39, 5311-5318.	10.0	79
72	Iron Isotope Fractionation during Pedogenesis in Redoximorphic Soils. Soil Science Society of America Journal, 2007, 71, 1840-1850.	2.2	79

#	Article	IF	CITATIONS
73	Effect of citrate on the local Fe coordination in ferrihydrite, arsenate binding, and ternary arsenate complex formation. Geochimica Et Cosmochimica Acta, 2010, 74, 5574-5592.	3.9	79
74	Heavy Metal Release from Contaminated Soils. Journal of Environmental Quality, 2003, 32, 865-875.	2.0	79
75	Photoreductive Dissolution of Iron(III) (Hydr)oxides in the Absence and Presence of Organic Ligands: Experimental Studies and Kinetic Modeling. Environmental Science & Technology, 2009, 43, 1864-1870.	10.0	76
76	Biogeochemical processes and arsenic enrichment around rice roots in paddy soil: results from micro-focused X-ray spectroscopy. European Journal of Soil Science, 2011, 62, 305-317.	3.9	76
77	Mercury Isotope Signatures in Contaminated Sediments as a Tracer for Local Industrial Pollution Sources. Environmental Science & amp; Technology, 2015, 49, 177-185.	10.0	75
78	Redox transformation, solid phase speciation and solution dynamics of copper during soil reduction and reoxidation as affected by sulfate availability. Geochimica Et Cosmochimica Acta, 2013, 123, 385-402.	3.9	73
79	Iron Isotope Fractionation during Fe Uptake and Translocation in Alpine Plants. Environmental Science & Technology, 2010, 44, 6144-6150.	10.0	72
80	Polymerization of Silicate on Hematite Surfaces and Its Influence on Arsenic Sorption. Environmental Science & amp; Technology, 2012, 46, 13235-13243.	10.0	71
81	Temperature-dependent formation of metallic copper and metal sulfide nanoparticles during flooding of a contaminated soil. Geochimica Et Cosmochimica Acta, 2013, 103, 316-332.	3.9	71
82	Characterization of dissolved organic matter in anoxic rock extracts and in situ pore water of the Opalinus Clay. Applied Geochemistry, 2007, 22, 2926-2939.	3.0	70
83	Arsenic Dynamics in Porewater of an Intermittently Irrigated Paddy Field in Bangladesh. Environmental Science & Technology, 2011, 45, 971-976.	10.0	70
84	Arsenic Accumulation in a Paddy Field in Bangladesh: Seasonal Dynamics and Trends over a Three-Year Monitoring Period. Environmental Science & Technology, 2010, 44, 2925-2931.	10.0	69
85	Mercury Isotope Signatures as Tracers for Hg Cycling at the New Idria Hg Mine. Environmental Science & Technology, 2013, 47, 6137-6145.	10.0	69
86	Spatial Distribution and Speciation of Arsenic in Peat Studied with Microfocused X-ray Fluorescence Spectrometry and X-ray Absorption Spectroscopy. Environmental Science & Technology, 2013, 47, 9706-9714.	10.0	69
87	Impact of Birnessite on Arsenic and Iron Speciation during Microbial Reduction of Arsenic-Bearing Ferrihydrite. Environmental Science & Technology, 2014, 48, 11320-11329.	10.0	69
88	Iron(II)-Catalyzed Iron Atom Exchange and Mineralogical Changes in Iron-rich Organic Freshwater Flocs: An Iron Isotope Tracer Study. Environmental Science & Technology, 2017, 51, 6897-6907.	10.0	69
89	Ferrihydrite Growth and Transformation in the Presence of Ferrous Iron and Model Organic Ligands. Environmental Science & Technology, 2019, 53, 13636-13647.	10.0	68
90	Influence of Arsenate Adsorption to Ferrihydrite, Goethite, and Boehmite on the Kinetics of Arsenate Reduction by <i>Shewanella putrefaciens</i> strain CN-32. Environmental Science & Technology, 2011, 45, 7701-7709.	10.0	67

#	Article	IF	CITATIONS
91	Source tracing of natural organic matter bound mercury in boreal forest runoff with mercury stable isotopes. Environmental Sciences: Processes and Impacts, 2017, 19, 1235-1248.	3.5	67
92	Sorption of Cu and Pb to kaolinite-fulvic acid colloids: Assessment of sorbent interactions. Geochimica Et Cosmochimica Acta, 2005, 69, 1675-1686.	3.9	66
93	Sequential Extraction Method for Speciation of Arsenate and Arsenite in Mineral Soils. Analytical Chemistry, 2010, 82, 5534-5540.	6.5	66
94	Reduction and Reoxidation of Humic Acid: Influence on Speciation of Cadmium and Silver. Environmental Science & Technology, 2012, 46, 8808-8816.	10.0	66
95	Copper Redox Transformation and Complexation by Reduced and Oxidized Soil Humic Acid. 1. X-ray Absorption Spectroscopy Study. Environmental Science & Technology, 2013, 47, 10903-10911.	10.0	66
96	Characterization of the pores in hydrous ferric oxide aggregates formed by freezing and thawing. Journal of Colloid and Interface Science, 2004, 271, 163-173.	9.4	65
97	Bacterial Siderophores Promote Dissolution of UO2under Reducing Conditions. Environmental Science & Technology, 2005, 39, 5709-5715.	10.0	65
98	Biotite alteration to halloysite and kaolinite in soil-saprolite profiles developed from mica schist and granite gneiss. Geoderma, 1997, 75, 155-170.	5.1	64
99	Isolation and characterization of dissolved organic matter from the Callovo–Oxfordian formation. Applied Geochemistry, 2007, 22, 1537-1548.	3.0	63
100	Iron speciation and isotope fractionation during silicate weathering and soil formation in an alpine glacier forefield chronosequence. Geochimica Et Cosmochimica Acta, 2011, 75, 5559-5573.	3.9	62
101	Microbial sulfate reduction decreases arsenic mobilization in flooded paddy soils with high potential for microbial Fe reduction. Environmental Pollution, 2019, 251, 952-960.	7.5	61
102	Time-Dependent Changes of Zinc Speciation in Four Soils Contaminated with Zincite or Sphalerite. Environmental Science & Technology, 2011, 45, 255-261.	10.0	60
103	Electrochemical Analysis of Changes in Iron Oxide Reducibility during Abiotic Ferrihydrite Transformation into Goethite and Magnetite. Environmental Science & Technology, 2019, 53, 3568-3578.	10.0	60
104	The Voltaic Effect as a Novel Mechanism Controlling the Remobilization of Cadmium in Paddy Soils during Drainage. Environmental Science & Technology, 2021, 55, 1750-1758.	10.0	59
105	Aggregation-dependent electron transfer via redox-active biochar particles stimulate microbial ferrihydrite reduction. Science of the Total Environment, 2020, 703, 135515.	8.0	57
106	Mercury Isotope Fractionation during Precipitation of Metacinnabar (β-HgS) and Montroydite (HgO). Environmental Science & Technology, 2015, 49, 4325-4334.	10.0	55
107	Tetra- and Hexavalent Uranium Forms Bidentate-Mononuclear Complexes with Particulate Organic Matter in a Naturally Uranium-Enriched Peatland. Environmental Science & Technology, 2016, 50, 10465-10475.	10.0	55
108	The within-field spatial variation in rice grain Cd concentration is determined by soil redox status and pH during grain filling. Environmental Pollution, 2020, 261, 114151.	7.5	55

#	Article	IF	CITATIONS
109	Iron and Arsenic Speciation and Distribution in Organic Flocs from Streambeds of an Arsenic-Enriched Peatland. Environmental Science & Technology, 2014, 48, 13218-13228.	10.0	52
110	Decreases in Iron Oxide Reducibility during Microbial Reductive Dissolution and Transformation of Ferrihydrite. Environmental Science & amp; Technology, 2019, 53, 8736-8746.	10.0	52
111	Slow Formation and Dissolution of Zn Precipitates in Soil:  A Combined Column-Transport and XAFS Study. Environmental Science & Technology, 2002, 36, 3749-3754.	10.0	51
112	Aggregation Kinetics of Kaoliniteâ^ Fulvic Acid Colloids as Affected by the Sorption of Cu and Pb. Environmental Science & Technology, 2005, 39, 807-813.	10.0	50
113	Weathering, soil formation and initial ecosystem evolution on a glacier forefield: a case study from the Damma Glacier, Switzerland. Mineralogical Magazine, 2008, 72, 19-22.	1.4	50
114	Chemical composition of aquatic dissolved organic matter in five boreal forest catchments sampled in spring and fall seasons. Biogeochemistry, 2006, 80, 263-275.	3.5	49
115	Photolysis of Citrate on the Surface of Lepidocrocite:  An in situ Attenuated Total Reflection Infrared Spectroscopy Study. Journal of Physical Chemistry C, 2007, 111, 10560-10569.	3.1	48
116	Kinetics of Hg(II) Exchange between Organic Ligands, Goethite, and Natural Organic Matter Studied with an Enriched Stable Isotope Approach. Environmental Science & Technology, 2014, 48, 13207-13217.	10.0	48
117	Sulfidization of Organic Freshwater Flocs from a Minerotrophic Peatland: Speciation Changes of Iron, Sulfur, and Arsenic. Environmental Science & Technology, 2016, 50, 3607-3616.	10.0	47
118	Zinc Fractionation in Contaminated Soils by Sequential and Single Extractions: Influence of Soil Properties and Zinc Content. Journal of Environmental Quality, 2008, 37, 1190-1200.	2.0	46
119	Solid Phase Speciation and Solubility of Vanadium in Highly Weathered Soils. Environmental Science & Technology, 2017, 51, 8254-8262.	10.0	46
120	Characterization of zinc in contaminated soils: complementary insights from isotopic exchange, batch extractions and XAFS spectroscopy. European Journal of Soil Science, 2011, 62, 318-330.	3.9	45
121	ATR-FTIR spectroscopic study of the adsorption of desferrioxamine B and aerobactin to the surface of lepidocrocite (I³-FeOOH). Geochimica Et Cosmochimica Acta, 2009, 73, 4661-4672.	3.9	44
122	Calcium isotope fractionation in alpine plants. Biogeochemistry, 2013, 112, 373-388.	3.5	44
123	Arsenic Species Formed from Arsenopyrite Weathering along a Contamination Gradient in Circumneutral River Floodplain Soils. Environmental Science & Technology, 2014, 48, 208-217.	10.0	44
124	Modelling sorption and mobility of cadmium and zinc in soils with scaled exchange coefficients. European Journal of Soil Science, 2003, 54, 387-400.	3.9	41
125	Vertical Distribution and Speciation of Trace Metals in Weathering Flotation Residues of a Zinc/Lead Sulfide Mine. Journal of Environmental Quality, 2007, 36, 61-69.	2.0	41
126	Multicomponent transport of major cations predicted from binary adsorption experiments. Journal of Contaminant Hydrology, 2000, 46, 319-338.	3.3	39

#	Article	IF	CITATIONS
127	Changes in Zn speciation during soil formation from Zn-rich limestones. Geochimica Et Cosmochimica Acta, 2009, 73, 5554-5571.	3.9	39
128	Mercury Mobilization in a Flooded Soil by Incorporation into Metallic Copper and Metal Sulfide Nanoparticles. Environmental Science & amp; Technology, 2013, 47, 7739-7746.	10.0	39
129	Effects of Manganese Oxide on Arsenic Reduction and Leaching from Contaminated Floodplain Soil. Environmental Science & Technology, 2016, 50, 9251-9261.	10.0	39
130	Impact of Organic Matter on Microbially-Mediated Reduction and Mobilization of Arsenic and Iron in Arsenic(V)-Bearing Ferrihydrite. Environmental Science & 201, 2021, 2021, 55, 1319-1328.	10.0	39
131	Cation Competition in a Natural Subsurface Material:Â Modeling of Sorption Equilibria. Environmental Science & Technology, 2000, 34, 2149-2155.	10.0	38
132	Local coordination of Zn in hydroxy-interlayered minerals and implications for Zn retention in soils. Geochimica Et Cosmochimica Acta, 2009, 73, 348-363.	3.9	38
133	Evolution of carbon fluxes during initial soil formation along the forefield of Damma glacier, Switzerland. Biogeochemistry, 2013, 113, 545-561.	3.5	38
134	Synthetic coprecipitates of exopolysaccharides and ferrihydrite. Part II: Siderophore-promoted dissolution. Geochimica Et Cosmochimica Acta, 2008, 72, 1128-1142.	3.9	37
135	Monothioarsenate Transformation Kinetics Determining Arsenic Sequestration by Sulfhydryl Groups of Peat. Environmental Science & amp; Technology, 2018, 52, 7317-7326.	10.0	37
136	Heavy Metal Release from Contaminated Soils. Journal of Environmental Quality, 2003, 32, 865.	2.0	35
137	Copper Redox Transformation and Complexation by Reduced and Oxidized Soil Humic Acid. 2. Potentiometric Titrations and Dialysis Cell Experiments. Environmental Science & Technology, 2013, 47, 10912-10921.	10.0	35
138	Sorption kinetics of strontium in porous hydrous ferric oxide aggregates II. Comparison of experimental results and model predictions. Journal of Colloid and Interface Science, 2005, 283, 29-40.	9.4	34
139	Mobility, turnover and storage of pollutants in soils, sediments and waters: achievements and results of the EU project AquaTerra. A review. Agronomy for Sustainable Development, 2009, 29, 161-173.	5.3	34
140	Filter Efficiency of Three Saprolites for Natural Clay and Iron Oxide Colloids. Environmental Science & Technology, 1994, 28, 1907-1915.	10.0	33
141	Small-scale studies of roasted ore waste reveal extreme ranges of stable mercury isotope signatures. Geochimica Et Cosmochimica Acta, 2014, 137, 1-17.	3.9	33
142	Nitrite Accumulation Is Required for Microbial Anaerobic Iron Oxidation, but Not for Arsenite Oxidation, in Two Heterotrophic Denitrifiers. Environmental Science & Technology, 2020, 54, 4036-4045.	10.0	33
143	Bioaccessibility of Arsenic in Mining-Impacted Circumneutral River Floodplain Soils. Environmental Science & Technology, 2014, 48, 13468-13477.	10.0	32
144	Stable Hg Isotope Signatures in Creek Sediments Impacted by a Former Hg Mine. Environmental Science & Technology, 2015, 49, 767-776.	10.0	32

#	Article	IF	CITATIONS
145	Mercury isotope signatures of digests and sequential extracts from industrially contaminated soils and sediments. Science of the Total Environment, 2018, 636, 1344-1354.	8.0	32
146	Low Concentrations of Surfactants Enhance Siderophore-Promoted Dissolution of Goethite. Environmental Science & Technology, 2007, 41, 3633-3638.	10.0	31
147	Photodissolution of lepidocrocite (γ-FeOOH) in the presence of desferrioxamine B and aerobactin. Geochimica Et Cosmochimica Acta, 2009, 73, 4673-4687.	3.9	31
148	A laboratory investigation of the ice nucleation efficiency of three types of mineral and soil dust. Atmospheric Chemistry and Physics, 2018, 18, 16515-16536.	4.9	31
149	Size Distribution of Organic Matter and Associated Propiconazole in Agricultural Runoff Material. Journal of Environmental Quality, 2003, 32, 2200-2206.	2.0	30
150	New Clues to the Local Atomic Structure of Short-Range Ordered Ferric Arsenate from Extended X-ray Absorption Fine Structure Spectroscopy. Environmental Science & Technology, 2013, 47, 3122-3131.	10.0	30
151	Oxidation of Organosulfur-Coordinated Arsenic and Realgar in Peat: Implications for the Fate of Arsenic. Environmental Science & amp; Technology, 2014, 48, 2281-2289.	10.0	29
152	Processes Governing Chromium Contamination of Groundwater and Soil from a Chromium Waste Source. ACS Earth and Space Chemistry, 2020, 4, 35-49.	2.7	29
153	Mineralogical Controls on the Bioaccessibility of Arsenic in Fe(III)–As(V) Coprecipitates. Environmental Science & Technology, 2018, 52, 616-627.	10.0	28
154	Mercury emission from industrially contaminated soils in relation to chemical, microbial, and meteorological factors. Environmental Pollution, 2019, 250, 944-952.	7.5	27
155	Speciation of Zn in Blast Furnace Sludge from Former Sedimentation Ponds Using Synchrotron X-ray Diffraction, Fluorescence, and Absorption Spectroscopy. Environmental Science & Technology, 2012, 46, 12381-12390.	10.0	26
156	Arsenite Binding to Sulfhydryl Groups in the Absence and Presence of Ferrihydrite: A Model Study. Environmental Science & Technology, 2014, 48, 3822-3831.	10.0	25
157	Interactions of ferrous iron with clay mineral surfaces during sorption and subsequent oxidation. Environmental Sciences: Processes and Impacts, 2020, 22, 1355-1367.	3.5	25
158	Arsenic redox transformations and cycling in the rhizosphere of Pteris vittata and Pteris quadriaurita. Environmental and Experimental Botany, 2020, 177, 104122.	4.2	25
159	Cyanide Leaching from Soil Developed from Coking Plant Purifier Waste as Influenced by Citrate. Vadose Zone Journal, 2004, 3, 471-479.	2.2	25
160	Stabilization of Ferrihydrite and Lepidocrocite by Silicate during Fe(II)-Catalyzed Mineral Transformation: Impact on Particle Morphology and Silicate Distribution. Environmental Science & Technology, 2022, 56, 5929-5938.	10.0	25
161	Reductive solubilization of arsenic in a mining-impacted river floodplain: Influence of soil properties and temperature. Environmental Pollution, 2017, 231, 722-731.	7.5	24
162	Copper Mobilization and Immobilization along an Organic Matter and Redox Gradient—Insights from a Mofette Site. Environmental Science & Technology, 2018, 52, 13698-13707.	10.0	23

#	Article	IF	CITATIONS
163	Organic matter influences transformation products of ferrihydrite exposed to sulfide. Environmental Science: Nano, 2020, 7, 3405-3418.	4.3	23
164	Aerobic Reduction of Chromium(VI) by <i>Pseudomonas corrugata</i> 28: Influence of Metabolism and Fate of Reduced Chromium. Geomicrobiology Journal, 2012, 29, 173-185.	2.0	22
165	Speciation and Mobility of Mercury in Soils Contaminated by Legacy Emissions from a Chemical Factory in the Rhône Valley in Canton of Valais, Switzerland. Soil Systems, 2018, 2, 44.	2.6	22
166	Microspectroscopy reveals dust-derived apatite grains in acidic, highly-weathered Hawaiian soils. Geoderma, 2021, 381, 114681.	5.1	22
167	Sorption kinetics of strontium in porous hydrous ferric oxide aggregates. Journal of Colloid and Interface Science, 2005, 283, 18-28.	9.4	21
168	Mineralisation and leaching of C from 13C labelled plant litter along an initial soil chronosequence of a glacier forefield. Soil Biology and Biochemistry, 2013, 57, 237-247.	8.8	21
169	Soil-to-plant transfer of arsenic and phosphorus along a contamination gradient in the mining-impacted Ogosta River floodplain. Science of the Total Environment, 2016, 572, 742-754.	8.0	21
170	Rate laws of steady-state and non-steady-state ligand-controlled dissolution of goethite. Colloids and Surfaces A: Physicochemical and Engineering Aspects, 2007, 306, 22-28.	4.7	20
171	Wavelength-Dependence of Photoreductive Dissolution of Lepidocrocite (Î ³ -FeOOH) in the Absence and Presence of the Siderophore DFOB. Environmental Science & Technology, 2009, 43, 1871-1876.	10.0	20
172	The genomic basis of adaptation to calcareous and siliceous soils in <i>Arabidopsis lyrata</i> . Molecular Ecology, 2018, 27, 5088-5103.	3.9	20
173	Two-year and multi-site field trials to evaluate soil amendments for controlling cadmium accumulation in rice grain. Environmental Pollution, 2021, 289, 117918.	7.5	20
174	Copper complexation of methanobactin isolated from Methylosinus trichosporium OB3b: pH-dependent speciation and modeling. Journal of Inorganic Biochemistry, 2012, 116, 55-62.	3.5	19
175	A coupled function of biochar as geobattery and geoconductor leads to stimulation of microbial Fe(III) reduction and methanogenesis in a paddy soil enrichment culture. Soil Biology and Biochemistry, 2021, 163, 108446.	8.8	19
176	X-ray Absorption and Emission Spectroscopy of CrIII (Hydr)Oxides: Analysis of the K-Pre-Edge Region. Journal of Physical Chemistry A, 2009, 113, 12171-12178.	2.5	18
177	Competitive ligand exchange between <scp><scp>Cu</scp>–humic acid complexes and methanobactin. Geobiology, 2013, 11, 44-54.</scp>	2.4	18
178	Mercury Reduction by Nanoparticulate Vivianite. Environmental Science & Technology, 2021, 55, 3399-3407.	10.0	18
179	Proton and Trivalent Metal Cation Binding by Dissolved Organic Matter in the Opalinus Clay and the Callovo-Oxfordian Formation. Environmental Science & Technology, 2008, 42, 5985-5991.	10.0	17
180	The Cr X-ray absorption K-edge structure of poorly crystalline Fe(III)-Cr(III)-oxyhydroxides. American Mineralogist, 2010, 95, 1202-1213.	1.9	17

6

#	Article	IF	CITATIONS
181	<i>Clostridium</i> Species as Metallic Copper-Forming Bacteria in Soil under Reducing Conditions. Geomicrobiology Journal, 2015, 32, 130-139.	2.0	17
182	The Effect of Aeration on Mn(II) Sorbed to Clay Minerals and Its Impact on Cd Retention. Environmental Science & Technology, 2021, 55, 1650-1658.	10.0	16
183	Surface precipitation of Mn ²⁺ on clay minerals enhances Cd ²⁺ sorption under anoxic conditions. Environmental Sciences: Processes and Impacts, 2020, 22, 1654-1665.	3.5	15
184	Carbon group chemistry of humic and fulvic acid: A comparison of C-1s NEXAFS and 13C-NMR spectroscopies. , 0, , 39-48.		14
185	Cation competition in a natural subsurface material: Prediction of transport behavior. Water Resources Research, 2002, 38, 7-1-7-7.	4.2	14
186	Effects of anionic surfactants on ligand-promoted dissolution of iron and aluminum hydroxides. Journal of Colloid and Interface Science, 2008, 321, 279-287.	9.4	14
187	Response to Comment on "New Clues to the Local Atomic Structure of Short-Range Ordered Ferric Arsenate from Extended X-ray Absorption Fine Structure Spectroscopy― Environmental Science & Technology, 2013, 47, 13201-13202.	10.0	14
188	Isolation and purification of Cu-free methanobactin from Methylosinus trichosporiumOB3b. Geochemical Transactions, 2011, 12, 2.	0.7	13
189	Effect of NOM on copper sulfide nanoparticle growth, stability, and oxidative dissolution. Environmental Science: Nano, 2020, 7, 1163-1178.	4.3	11
190	How electron flow controls contaminant dynamics. Environmental Science & Technology, 2010, 44, 3-6.	10.0	10
191	Leaching of hexavalent chromium from young chromite ore processing residue. Journal of Environmental Quality, 2020, 49, 712-722.	2.0	10
192	Modeling Competitive Sorption and Release of Heavy Metals in Soils. , 2001, , 55-88.		8
193	Mineral characterization and composition of Fe-rich flocs from wetlands of Iceland: Implications for Fe, C and trace element export. Science of the Total Environment, 2022, 816, 151567.	8.0	8
194	Microbial Fe cycling in a simulated Precambrian ocean environment: Implications for secondary mineral (trans)formation and deposition during BIF genesis. Geochimica Et Cosmochimica Acta, 2022, 331, 165-191.	3.9	8
195	Cyanide Leaching from Soil Developed from Coking Plant Purifier Waste as Influenced by Citrate. Vadose Zone Journal, 2004, 3, 471-479.	2.2	7
196	Effects of natural organic matter (NOM), metal-to-sulfide ratio and Mn2+on cadmium sulfide nanoparticle growth and colloidal stability. Environmental Science: Nano, 2020, 7, 3385-3404.	4.3	7
197	Adsorption of hydroxamate siderophores and EDTA on goethite in the presence of the surfactant sodium dodecyl sulfate. Geochemical Transactions, 2009, 10, 5.	0.7	6

198 Chemical Properties and Processes. , 2016, , 123-174.

#	Article	IF	CITATIONS
199	Plant Availability of Zinc and Copper in Soil after Contamination with Brass Foundry Filter Dust. Journal of Environmental Quality, 2007, 36, 44-52.	2.0	5
200	Origin of high Zn contents in Jurassic limestone of the Jura mountain range and the Burgundy: evidence from Zn speciation and distribution. Swiss Journal of Geosciences, 2011, 104, 409-424.	1.2	5
201	Copper mobilisation from Cu sulphide minerals by methanobactin: Effect of <scp>pH</scp> , oxygen and natural organic matter. Geobiology, 2022, 20, 690-706.	2.4	5
202	Exploring Key Soil Parameters Relevant to Arsenic and Cadmium Accumulation in Rice Grain in Southern China. Soil Systems, 2022, 6, 36.	2.6	4
203	Entwicklung eines Computerverfahrens zur Berechnung der hydraulischen LeitfĤigkeit von wassergesĤtigten Böden mit der Bohrlochmethode. Zeitschrift Fur Pflanzenernahrung Und Bodenkunde = Journal of Plant Nutrition and Plant Science, 1989, 152, 17-20.	0.4	2
204	Synchrotron-based Spectroscopy Reveals First Evidence for Organic Sulfur-coordinated Arsenic in Peat. Chimia, 2012, 66, 877-877.	0.6	2
205	Effect of extreme metal(loid) concentrations on prokaryotic community structure in floodplain soils contaminated with mine waste. Applied Soil Ecology, 2019, 144, 182-195.	4.3	2
206	New methods for the environmental chemist's toolbox. Environmental Science & Technology, 2008, 42, 7727-7727.	10.0	1
207	Chemische Eigenschaften und Prozesse. , 2010, , 121-170.		1
208	Chemische Eigenschaften und Prozesse. , 2010, , 121-170.		1
209	An American in Zurich: Jerry Schnoor as an Ambassador for U.S. Environmental Science and Engineering. Environmental Science & Technology, 2016, 50, 6597-6598.	10.0	0
210	Proton and metal cation binding to humic substances in relation to chemical composition and molecular size. , 0, , 153-164.		0